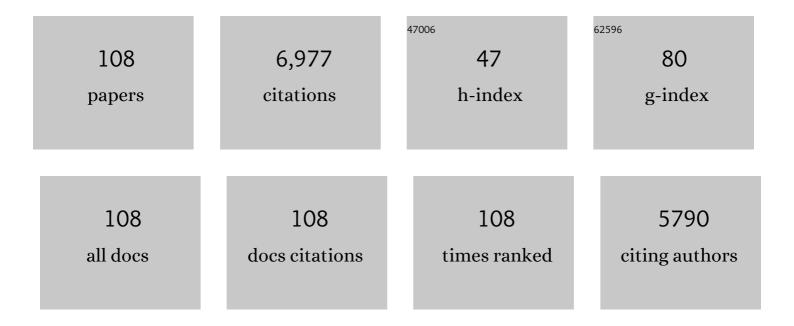
Tong Zhang

List of Publications by Year in descending order

Source: https://exaly.com/author-pdf/3684101/publications.pdf Version: 2024-02-01



ΤΟΝΟ ΖΗΛΝΟ

#	Article	IF	CITATIONS
1	SnO2 nanoparticles-reduced graphene oxide nanocomposites for NO2 sensing at low operating temperature. Sensors and Actuators B: Chemical, 2014, 190, 472-478.	7.8	429
2	Enhancing NO2 gas sensing performances at room temperature based on reduced graphene oxide-ZnO nanoparticles hybrids. Sensors and Actuators B: Chemical, 2014, 202, 272-278.	7.8	322
3	An overview: Facet-dependent metal oxide semiconductor gas sensors. Sensors and Actuators B: Chemical, 2018, 277, 604-633.	7.8	286
4	Direct Writing on Paper of Foldable Capacitive Touch Pads with Silver Nanowire Inks. ACS Applied Materials & Interfaces, 2014, 6, 21721-21729.	8.0	220
5	Metal–Organic Frameworks-Derived Hierarchical Co ₃ O ₄ Structures as Efficient Sensing Materials for Acetone Detection. ACS Applied Materials & Interfaces, 2018, 10, 9765-9773.	8.0	215
6	Ultrafast Response Polyelectrolyte Humidity Sensor for Respiration Monitoring. ACS Applied Materials & Interfaces, 2019, 11, 6483-6490.	8.0	201
7	P-type Co3O4 nanomaterials-based gas sensor: Preparation and acetone sensing performance. Sensors and Actuators B: Chemical, 2017, 242, 369-377.	7.8	184
8	Recent Progress of Nanostructured Sensing Materials from 0D to 3D: Overview of Structure–Propertyâ€Application Relationship for Gas Sensors. Small Methods, 2021, 5, e2100515.	8.6	162
9	A humidity sensor based on KCl-doped SnO2 nanofibers. Sensors and Actuators B: Chemical, 2009, 138, 368-373.	7.8	153
10	Construction of ZnO/SnO ₂ Heterostructure on Reduced Graphene Oxide for Enhanced Nitrogen Dioxide Sensitive Performances at Room Temperature. ACS Sensors, 2019, 4, 2048-2057.	7.8	142
11	Cross-linked p-type Co3O4 octahedral nanoparticles in 1D n-type TiO2 nanofibers for high-performance sensing devices. Journal of Materials Chemistry A, 2014, 2, 10022.	10.3	135
12	Synthesis and toluene sensing properties of SnO2 nanofibers. Sensors and Actuators B: Chemical, 2009, 137, 471-475.	7.8	127
13	Preparation of Ag nanoparticles-SnO2 nanoparticles-reduced graphene oxide hybrids and their application for detection of NO2 at room temperature. Sensors and Actuators B: Chemical, 2016, 222, 893-903.	7.8	122
14	High performance room temperature NO2 sensors based on reduced graphene oxide-multiwalled carbon nanotubes-tin oxide nanoparticles hybrids. Sensors and Actuators B: Chemical, 2015, 211, 318-324.	7.8	111
15	Hollow ZnSnO ₃ Cubes with Controllable Shells Enabling Highly Efficient Chemical Sensing Detection of Formaldehyde Vapors. ACS Applied Materials & Interfaces, 2017, 9, 14525-14533.	8.0	110
16	Oxygen vacancy engineering for enhanced sensing performances: A case of SnO2 nanoparticles-reduced graphene oxide hybrids for ultrasensitive ppb-level room-temperature NO2 sensing. Sensors and Actuators B: Chemical, 2018, 266, 812-822.	7.8	109
17	Drawn on Paper: A Reproducible Humidity Sensitive Device by Handwriting. ACS Applied Materials & Interfaces, 2017, 9, 28002-28009.	8.0	104
18	Investigation of Microstructure Effect on NO ₂ Sensors Based on SnO ₂ Nanoparticles/Reduced Graphene Oxide Hybrids. ACS Applied Materials & Interfaces, 2018, 10, 41773-41783.	8.0	100

#	Article	IF	CITATIONS
19	High-performance reduced graphene oxide-based room-temperature NO2 sensors: A combined surface modification of SnO2 nanoparticles and nitrogen doping approach. Sensors and Actuators B: Chemical, 2017, 242, 269-279.	7.8	99
20	Design of Core–Shell Heterostructure Nanofibers with Different Work Function and Their Sensing Properties to Trimethylamine. ACS Applied Materials & Interfaces, 2016, 8, 19799-19806.	8.0	93
21	A formaldehyde sensor: Significant role of p-n heterojunction in gas-sensitive core-shell nanofibers. Sensors and Actuators B: Chemical, 2018, 258, 1230-1241.	7.8	93
22	TiO2 nanostructures with different crystal phases for sensitive acetone gas sensors. Journal of Colloid and Interface Science, 2022, 607, 357-366.	9.4	93
23	Humidity sensing properties of KCl-doped ZnO nanofibers with super-rapid response and recovery. Sensors and Actuators B: Chemical, 2009, 137, 649-655.	7.8	91
24	Nanoparticles-assembled Co3O4 nanorods p-type nanomaterials: One-pot synthesis and toluene-sensing properties. Sensors and Actuators B: Chemical, 2014, 201, 1-6.	7.8	90
25	Ultra-sensitive sensing platform based on Pt-ZnO-In2O3 nanofibers for detection of acetone. Sensors and Actuators B: Chemical, 2018, 272, 185-194.	7.8	90
26	Template-assisted self-assembly method to prepare three-dimensional reduced graphene oxide for dopamine sensing. Sensors and Actuators B: Chemical, 2014, 205, 120-126.	7.8	89
27	Selective ppb-level ozone gas sensor based on hierarchical branch-like In2O3 nanostructure. Sensors and Actuators B: Chemical, 2021, 336, 129612.	7.8	88
28	Synthesis of core–shell α-Fe ₂ O ₃ @NiO nanofibers with hollow structures and their enhanced HCHO sensing properties. Journal of Materials Chemistry A, 2015, 3, 5635-5641.	10.3	83
29	Flexible humidity sensor based on modified cellulose paper. Sensors and Actuators B: Chemical, 2021, 339, 129879.	7.8	83
30	Humidity sensors based on Li-loaded nanoporous polymers. Sensors and Actuators B: Chemical, 2014, 190, 523-528.	7.8	81
31	Facile preparation of hierarchical structure based on p-type Co3O4 as toluene detecting sensor. Applied Surface Science, 2020, 503, 144167.	6.1	81
32	Ordered mesoporous Co3O4 for high-performance toluene sensing. Sensors and Actuators B: Chemical, 2014, 197, 342-349.	7.8	78
33	Horseshoe-shaped SnO2 with annulus-like mesoporous for ethanol gas sensing application. Sensors and Actuators B: Chemical, 2017, 240, 1321-1329.	7.8	76
34	Effect of Cation Substitution on the Gas-Sensing Performances of Ternary Spinel MCo ₂ O ₄ (M = Mn, Ni, and Zn) Multishelled Hollow Twin Spheres. ACS Applied Materials & Interfaces, 2019, 11, 28023-28032.	8.0	76
35	MOF–Derived 1 D α–Fe2O3/NiFe2O4 heterojunction as efficient sensing materials of acetone vapors. Sensors and Actuators B: Chemical, 2019, 281, 885-892.	7.8	75
36	Sulfonated graphene anchored with tin oxide nanoparticles for detection of nitrogen dioxide at room temperature with enhanced sensing performances. Sensors and Actuators B: Chemical, 2016, 228, 134-143.	7.8	73

#	Article	IF	CITATIONS
37	Study on highly selective sensing behavior of ppb-level oxidizing gas sensors based on Zn2SnO4 nanoparticles immobilized on reduced graphene oxide under humidity conditions. Sensors and Actuators B: Chemical, 2019, 285, 590-600.	7.8	70
38	NiO/NiCo ₂ O ₄ Truncated Nanocages with PdO Catalyst Functionalization as Sensing Layers for Acetone Detection. ACS Applied Materials & Interfaces, 2018, 10, 37242-37250.	8.0	69
39	Design strategy for ultrafast-response humidity sensors based on gel polymer electrolytes and application for detecting respiration. Sensors and Actuators B: Chemical, 2020, 304, 127270.	7.8	66
40	Proton-Conductive Gas Sensor: a New Way to Realize Highly Selective Ammonia Detection for Analysis of Exhaled Human Breath. ACS Sensors, 2020, 5, 346-352.	7.8	66
41	Structure-driven efficient NiFe2O4 materials for ultra-fast response electronic sensing platform. Sensors and Actuators B: Chemical, 2018, 255, 1436-1444.	7.8	65
42	A QCM humidity sensor constructed by graphene quantum dots and chitosan composites. Sensors and Actuators A: Physical, 2019, 287, 93-101.	4.1	64
43	Chitosan wrapped multiwalled carbon nanotubes as quartz crystal microbalance sensing material for humidity detection. Journal of Colloid and Interface Science, 2020, 560, 284-292.	9.4	63
44	Comparison of toluene sensing performances of zinc stannate with different morphology-based gas sensors. Sensors and Actuators B: Chemical, 2016, 227, 448-455.	7.8	62
45	Preparation of crumpled reduced graphene oxide–poly(p-phenylenediamine) hybrids for the detection of dopamine. Journal of Materials Chemistry A, 2013, 1, 13314.	10.3	60
46	Anchoring ultrafine Pd nanoparticles and SnO2 nanoparticles on reduced graphene oxide for high-performance room temperature NO2 sensing. Journal of Colloid and Interface Science, 2018, 514, 599-608.	9.4	60
47	Hierarchical structure with heterogeneous phase as high performance sensing materials for trimethylamine gas detecting. Sensors and Actuators B: Chemical, 2015, 220, 1224-1231.	7.8	55
48	Oxygen vacancy modulation of commercial SnO2 by an organometallic chemistry-assisted strategy for boosting acetone sensing performances. Sensors and Actuators B: Chemical, 2019, 290, 493-502.	7.8	52
49	Study on humidity sensing property based on Li-doped mesoporous silica MCM-41. Sensors and Actuators B: Chemical, 2008, 133, 622-627.	7.8	47
50	Capacitive humidity sensors based on mesoporous silica and poly(3,4-ethylenedioxythiophene) composites. Journal of Colloid and Interface Science, 2020, 565, 592-600.	9.4	46
51	Humidity sensors based on MCM-41/polypyrrole hybrid film via in-situ polymerization. Sensors and Actuators B: Chemical, 2018, 277, 584-590.	7.8	44
52	One-dimensional porous Co3O4 rectangular rods for enhanced acetone gas sensing properties. Sensors and Actuators B: Chemical, 2019, 297, 126746.	7.8	44
53	Constructing Hierarchical Heterostructured Mn ₃ O ₄ /Zn ₂ SnO ₄ Materials for Efficient Gas Sensing Reaction. Advanced Materials Interfaces, 2018, 5, 1800115.	3.7	42
54	Room temperature ammonia gas sensor based on ionic conductive biomass hydrogels. Sensors and Actuators B: Chemical, 2020, 320, 128318.	7.8	42

#	Article	IF	CITATIONS
55	Rapid sensitive sensing platform based on yolk-shell hybrid hollow sphere for detection of ethanol. Sensors and Actuators B: Chemical, 2018, 256, 479-487.	7.8	40
56	Rational design and tunable synthesis of Co3O4 nanoparticle-incorporating into In2O3 one-dimensional ribbon as effective sensing material for gas detection. Sensors and Actuators B: Chemical, 2020, 310, 127695.	7.8	40
57	Humidity-activated ammonia sensor with excellent selectivity for exhaled breath analysis. Sensors and Actuators B: Chemical, 2021, 334, 129625.	7.8	40
58	The effect of different crystalline phases of In2O3 on the ozone sensing performance. Journal of Hazardous Materials, 2021, 418, 126290.	12.4	40
59	Fast and real-time acetone gas sensor using hybrid ZnFe ₂ O ₄ /ZnO hollow spheres. RSC Advances, 2016, 6, 66738-66744.	3.6	37
60	Preparation of organic-inorganic hybrid polymers and their humidity sensing properties. Sensors and Actuators B: Chemical, 2017, 242, 1108-1114.	7.8	37
61	A flexible humidity sensor based on self-supported polymer film. Sensors and Actuators B: Chemical, 2022, 358, 131438.	7.8	36
62	Constructing one dimensional Co3O4 hierarchical nanofibers as efficient sensing materials for rapid acetone gas detection. Journal of Alloys and Compounds, 2019, 799, 513-520.	5.5	35
63	Flexible Piezoresistive Sensors based on Conducting Polymer-coated Fabric Applied to Human Physiological Signals Monitoring. Journal of Bionic Engineering, 2020, 17, 55-63.	5.0	33
64	High-Performance QCM Humidity Sensors Using Acidized-Multiwalled Carbon Nanotubes as Sensing Film. IEEE Sensors Journal, 2018, 18, 5278-5283.	4.7	32
65	Facile construction of Co3O4 porous microspheres with enhanced acetone gas sensing performances. Materials Science in Semiconductor Processing, 2019, 101, 10-15.	4.0	32
66	Cabbage-shaped zinc-cobalt oxide (ZnCo2O4) sensing materials: Effects of zinc ion substitution and enhanced formaldehyde sensing properties. Journal of Colloid and Interface Science, 2019, 537, 520-527.	9.4	30
67	Study on a quartz crystal microbalance sensor based on chitosan-functionalized mesoporous silica for humidity detection. Journal of Colloid and Interface Science, 2021, 583, 340-350.	9.4	30
68	Porous Co3O4 nanocrystals derived by metal-organic frameworks on reduced graphene oxide for efficient room-temperature NO2 sensing properties. Journal of Alloys and Compounds, 2021, 856, 158199.	5.5	30
69	Improvement of gas sensing performance for tin dioxide sensor through construction of nanostructures. Journal of Colloid and Interface Science, 2019, 557, 673-682.	9.4	29
70	Electrochemical chloramphenicol sensors-based on trace MoS2 modified carbon nanomaterials: Insight into carbon supports. Journal of Alloys and Compounds, 2021, 872, 159687.	5.5	29
71	Boosting room-temperature ppb-level NO2 sensing over reduced graphene oxide by co-decoration of α-Fe2O3 and SnO2 nanocrystals. Journal of Colloid and Interface Science, 2022, 612, 689-700.	9.4	29
72	A dual-functional polyaniline film-based flexible electrochemical sensor for the detection of pH and lactate in sweat of the human body. Talanta, 2022, 242, 123289.	5.5	28

#	Article	IF	CITATIONS
73	Carbon materials-functionalized tin dioxide nanoparticles toward robust, high-performance nitrogen dioxide gas sensor. Journal of Colloid and Interface Science, 2018, 524, 76-83.	9.4	27
74	A yolk-double-shelled heterostructure-based sensor for acetone detecting application. Journal of Colloid and Interface Science, 2019, 539, 490-496.	9.4	27
75	Humidity sensor using a Li-loaded microporous organic polymer assembled by 1,3,5-trihydroxybenzene and terephthalic aldehyde. RSC Advances, 2014, 4, 28451.	3.6	26
76	Controllable construction of multishelled p-type cuprous oxide with enhanced formaldehyde sensing. Journal of Colloid and Interface Science, 2019, 535, 58-65.	9.4	25
77	A Composite Structure of <italic>In Situ</italic> Cross-Linked Poly(Ionic Liquid)s and Paper for Humidity-Monitoring Applications. IEEE Sensors Journal, 2019, 19, 833-837.	4.7	24
78	Dominant Role of Heterojunctions in Gas Sensing with Composite Materials. ACS Applied Materials & Interfaces, 2020, 12, 21127-21132.	8.0	24
79	An organometallic chemistry-assisted strategy for modification of zinc oxide nanoparticles by tin oxide nanoparticles: Formation of n-n heterojunction and boosting NO2 sensing properties. Journal of Colloid and Interface Science, 2020, 567, 328-338.	9.4	23
80	Development of solution processible organic-inorganic hybrid materials with core-shell framework for humidity monitoring. Sensors and Actuators B: Chemical, 2018, 255, 2878-2885.	7.8	22
81	Functionalization of Hybrid 1D SnO ₂ –ZnO Nanofibers for Formaldehyde Detection. Advanced Materials Interfaces, 2018, 5, 1800967.	3.7	22
82	Zn _x Co _{3â^'x} O ₄ bimetallic oxides derived from metal–organic frameworks for enhanced acetone sensing performances. Inorganic Chemistry Frontiers, 2019, 6, 3177-3183.	6.0	22
83	Hydrogen bonds-induced room-temperature detection of DMMP based on polypyrrole-reduced graphene oxide hybrids. Sensors and Actuators B: Chemical, 2021, 346, 130518.	7.8	22
84	Self-assembly polyaniline films for the high-performance ammonia gas sensor. Sensors and Actuators B: Chemical, 2022, 365, 131928.	7.8	21
85	Investigation of the effect of oxygen-containing groups on reduced graphene oxide-based room-temperature NO2 sensor. Journal of Alloys and Compounds, 2019, 801, 142-150.	5.5	20
86	Preparation of hydrophilic organic groups modified mesoporous silica materials and their humidity sensitive properties. Sensors and Actuators B: Chemical, 2017, 240, 681-688.	7.8	19
87	Humidity Sensors Based on 3D Porous Polyelectrolytes via Breath Figure Method. Advanced Electronic Materials, 2020, 6, 1900846.	5.1	19
88	The synergistic effects of oxygen vacancy engineering and surface gold decoration on commercial SnO2 for ppb-level DMMP sensing. Journal of Colloid and Interface Science, 2022, 608, 2703-2717.	9.4	19
89	Study on humidity sensitive property of K2CO3-SBA-15 composites. Applied Surface Science, 2009, 256, 280-283.	6.1	18
90	Humidity sensors based on metal organic frameworks derived polyelectrolyte films. Journal of Colloid and Interface Science, 2021, 602, 646-653.	9.4	17

#	Article	IF	CITATIONS
91	The synergistic effects of MoS2 and reduced graphene oxide on sensing performances for electrochemical chloramphenicol sensor. FlatChem, 2022, 33, 100364.	5.6	17
92	A universal sugar-blowing approach to synthesize fluorescent nitrogen-doped carbon nanodots for detection of Hg(II). Applied Surface Science, 2021, 544, 148725.	6.1	16
93	Nanosheet-assembled In2O3 for sensitive and selective ozone detection at low temperature. Journal of Alloys and Compounds, 2021, 888, 161430.	5.5	14
94	Glucose-assisted combustion synthesis of oxygen vacancy enriched α-MoO3 for ethanol sensing. Journal of Alloys and Compounds, 2022, 902, 163711.	5.5	14
95	A flexible electrochemical biosensor based on functionalized poly(3,4-ethylenedioxythiophene) film to detect lactate in sweat of the human body. Journal of Colloid and Interface Science, 2022, 617, 454-462.	9.4	12
96	Robust cobalt perforated with multi-walled carbon nanotubes as an effective sensing material for acetone detection. Inorganic Chemistry Frontiers, 2018, 5, 2563-2570.	6.0	11
97	Humidity Sensor Preparation by <italic>In Situ</italic> Click Polymerization. IEEE Electron Device Letters, 2018, 39, 1234-1237.	3.9	11
98	Highly Sensitive and Selective Dopamine Detection Utilizing Nitrogenâ€Doped Mesoporous Carbon Prepared by a Molten Glucoseâ€Assisted Hardâ€Template Approach. ChemPlusChem, 2019, 84, 845-852.	2.8	11
99	Mesoporous Magnesium Oxide Nanosheet Electrocatalysts for the Detection of Lead(II). ACS Applied Nano Materials, 2019, 2, 2606-2611.	5.0	11
100	In Situ Preparation of Porous Humidity Sensitive Composite via a One-Stone-Two-Birds Strategy. Sensors and Actuators B: Chemical, 2020, 316, 128159.	7.8	11
101	The effect of shell thickness on gas sensing properties of core-shell fibers. Sensors and Actuators B: Chemical, 2021, 332, 129456.	7.8	11
102	Controllably fabricated single microwires from Pd-WO3•xH2O nanoparticles by femtosecond laser for faster response ammonia sensors at room temperature. Sensors and Actuators B: Chemical, 2020, 316, 128122	7.8	10
103	altimg="si2.svg"><'mml:mrow> <mml:mfenced <br="" close="}">open="{"><mml:mrow><mml:mn>0001</mml:mn></mml:mrow></mml:mfenced> and <mml:math <br="" xmlns:mml="http://www.w3.org/1998/Math/MathML">altimg="si3.svg"><mml:mrow><mml:mfenced <="" close="}" td=""><td>2.6</td><td>9</td></mml:mfenced></mml:mrow></mml:math>	2.6	9
104	open="("> <mmtmrow><mmtmn>10</mmtmn><mmtmover><mmtmn>1Optical Waveguide Sensors for Measuring Human Temperature and Humidity with Gel Polymer Electrolytes. ACS Applied Materials & amp; Interfaces, 2021, 13, 60384-60392.</mmtmn></mmtmover></mmtmrow>	nml:mover 8.0	> <mml:mn> 9</mml:mn>
105	Sb/Pd co-doped SnO ₂ nanoparticles for methane detection: resistance reduction and sensing performance studies. Nanotechnology, 2021, 32, 475506.	2.6	8
106	A Flexible Pressure Sensor Based on Bimaterial Conductivity-Conversion Mechanism. IEEE Electron Device Letters, 2021, 42, 1857-1860.	3.9	6
107	Study on a Humidity Sensor of Quartz Crystal Microbalance Modified With Multi-Pore Polydopamine. IEEE Electron Device Letters, 2022, 43, 611-614.	3.9	6
108	High Sensitive Humidity Sensors Based on Biomass Ionogels. IEEE Sensors Journal, 2022, 22, 12570-12575.	4.7	5